Desalination and Water Treatment
www.deswater.com
doi: 10.5004/dwt.2018.22683

123 (2018) 203–210
August

Mesoporosity development in zeolite beta by using desilication and CTAB assembly for removal of Mn^{2+}

Seo-Hyun Pak[a], Chan-Gyu Park[a,*], Gwang Nam Kang[b], Young-hee Kim[c,d]

[a]*Environmental Technology Division, Korea Testing Laboratory, 87, Digital-ro 26-gil, Guro-gu, Seoul 08389, Korea, Tel. +82 2-860-1105, +82 2-860-1139; Fax: +82-02-860-1689; emails: pcg6189@hotmail.com, seohyunpak@ktl.re.kr (S.-H. Pak), Tel. +82 2-860-1272; Fax: +82 2-860-1689; email: pcg6189@hotmail.com (C.-G. Park)*
[b]*ATE Corp., 551-24, Yangcheon-ro, Gangseo-gu, Seoul, South Korea*
[c]*ILSHIN Environmental Engineering Co., Ltd., A-1111, Munjeong Hyundai Knowledge Industry Center, #11, Beobwon-ro 11-gil, Sonpa-gu, Seoul 05836, Korea*
[d]*Hoseo Graduate School of Venture, Banpo-daero 9-gil, Seocho-gu, Seoul 06711, Korea*

Received 25 October 2017; Accepted 26 June 2018

ABSTRACT

Mesoporous zeolite beta (Si/Al = 25) was synthesized in an aqueous 2–7 M NaOH solution and cetyltrimethylammonium bromide (CTAB) (0.18 M) solution to form mesopores via the extraction of framework silicon and surfactant assembly. The physicochemical properties of the mesoporous zeolites beta were then analyzed using X-ray diffraction, nitrogen full isotherms at 77 K, scanning electron microscopy, transmission electron microscopy, ^{29}Si-nuclear magnetic resonance, and Fourier transform infrared spectroscopy. The commercial zeolite beta, −Si–O–Al–, and −Si–O–Si– linkages were broken due to the NaOH process. Micelles formed by CTAB then lead to the formation of mesoporosity with zeolite beta character. This material, which introduces mesoporosity into zeolite beta, displayed a superior adsorption capacity than commercial materials when used as an adsorbent for manganese removal.

Keywords: Mesoporosity; Desilication; CTAB; Zeolite; Zeolite beta; Water treatment; Manganese

1. Introduction

Excessive amounts of heavy metals can be harmful to human beings and can cause serious problems for plants and animals. There has been a rapid increase in the discharge of heavy metals such as cadmium, manganese, lead, mercury, and iron due to wastewater emissions. Typical ways to treat wastewater containing heavy metals are microfiltration [1], ultrafiltration [2], nanofiltration [3], adsorption (using activated carbon), and ion exchange [4]. Among these, the use of activated carbon and zeolites has been investigated extensively. Activated carbon is an adsorbent with varying pore sizes, which enable various contaminants to be adsorbed, but it is not selective. Zeolites, on the other hand, have uniform pore sizes and can selectively adsorb contaminants through a molecular sieve effect and an ion exchange function. While zeolites are less economical than activated carbon, the size and shape of the adsorption particles facilitate the separation and recovery of sorbents in heavy metal adsorption; therefore, it is worthwhile to research zeolites for use as absorbents.

Zeolites are a well-known group of crystalline (alumino) silicates that possess a unique combination of properties, including high surface area, well-defined hydrothermally stable framework, stability, and ability to confine active metal species in their pores at molecular dimensions of 0.3–1.5 nm. The micropores of zeolites display shape selectivity in various catalytic applications, but there are concerns regarding the restricted transport in these micropores due to diffusional limitations. Mesopores, created in microporous crystals (zeolites), enhance the diffusion rate by improving access of substrates to the micropores and shortening the diffusion path length [5].

* Corresponding author.

Various approaches have been designed for preparing mesoporous zeolites, such as direct synthesis, postsynthesis, zeolitization of mesoporous materials, and recrystallization of zeolites [6]. Direct synthesis has been applied to produce new mesoporous zeolites or hybrid materials that combine the advantages of microporous and mesoporous materials. Another process for the preparation of mesoporous zeolites involves a template method using porous carbon, aerogels, and other porous materials. Post-treatments leading to the removal of Al (de-alumination) or Si (desilication) have been applied to the synthesis of mesoporous zeolite [7–15]. Among these methods, desilication was initially applied to ZSM-5 structures in an alkaline solution [9,14].

Recrystallization is another process for preparing mesoporous zeolites. The most important feature of the recrystallization method is that mesoporous zeolites can be obtained through zeolite dissolution and reassembly, which find broad application as hierarchical materials. In addition, recrystallization mainly relies on the level of dissolution [6]. Among the various recrystallization methods, our strategy for preparing a micro/mesoporous composite is based on the assembly of surfactants and alkali-treated zeolite with small zeolitic fragments in the walls. Yan et al. [16] reported a beta/MCM-41 micro/mesoporous composite prepared via the assembly of zeolite beta seeding ($NaAlO_2$, TEAOH) with cetyltrimethylammonium bromide (CTAB). Another group studied mesoporous mordenite (MOR) obtained by a two-step procedure using NaOH and CTMABr [17,18].

Zeolite beta with mesoporosity was prepared by the recrystallization method in an alkaline solution (0.7–3 M) in the presence of CTAB [19]. Dou et al. [20] reported that mesoporous zeolite beta (Si/Al = 12.5) was synthesized by pH adjustment in NaOH (1 M) and CTAB at 373 K for 24 h.

Herein, we present a process to synthesize micro/mesoporous zeolite beta via the self-assembly of zeolite beta particles or their hydrolysis products based on the NaOH treatment (2–7 M) of commercial beta zeolite (Si/Al = 25) and CTAB under stirring with pH adjustment (pH 10). The ability of micro/mesoporous zeolite beta to adsorb Mn^{2+} was studied. To date, there is hardly any report on the synthesis and optimization of commercial zeolite beta, prepared in a NaOH alkaline solution with CTAB assembly, for the removal of heavy metal.

In this work, alkaline NaOH treatment of commercial zeolite beta using a surfactant assembly is proposed as a promising alternative to increase the porosity of zeolites while preserving zeolite characteristics such as crystallinity and microporosity. Focus was placed on the optimization of the mesoporous beta structure by varying the NaOH concentration and the application of this zeolite for adsorbing metal in water.

2. Experimental procedure

2.1. Chemicals

A commercial synthetic zeolite beta (Si/Al = 25) in powder form was purchased from Alfa Aesar, USA. NaOH and CTAB were purchased from SAMCHUN, Korea and used without purification. Ammonium chloride and acetic acid (ACS reagent grade, ≥99.7%) were purchased from Sigma-Aldrich, USA and used without purification.

2.2. Synthesis

- Preparation of zeolite beta precursors: NaOH solutions (2–7 M) were prepared and mixed with 16.87 g of commercial zeolite beta (ZB, Si/Al = 25). The solutions were then stirred at 35°C for 1 h to obtain a viscous solution, referred to as "beta-precursors."
- pH adjustments and crystallization: 570 mL of CTAB solution (0.18 M) was added to the prepared beta-precursors and stirred for 2 h at 40°C. Next, the pH of the solutions was adjusted to 10.0 using a 50 wt% acetic acid solution and the solutions were aged at 102°C for 18 h. The pH adjustment and aging steps were repeated three times.
- The powder resulting from Step (2) was suction-filtered and thoroughly washed with ethanol and water. The powder was calcined at 450°C for 4 h to remove the template.
- Ion exchange: NH_4^+ foam of mesoporous zeolite beta was obtained by repeated ion exchange with 1 M NH_4Cl for 2 h at 60°C. The protonated form was then obtained by calcining the NH_4^+ foam at 500°C for 4 h.

2.3. Characterization

X-ray diffraction (XRD) patterns of the mesoporous zeolite betas were obtained using PANalytical's X-ray diffractometers (anode material = Cu; K_α radiation = 20 mA; 45 kV). Low-angle XRD patterns were collected in the range of 2θ = 0.51°–9.99° at a scanning step time of 5 s. High-angle XRD patterns were collected in the range of 2θ = 5°–90° at a scanning step time of 29.84 s. The morphologies and pore structures of mesoporous zeolite betas were verified using scanning electron microscopy (630-F microscope, JEOL, Japan) and transmission electron microscopy (TEM; JEM-2100F, JEOL, Japan). The adsorption–desorption isotherms of nitrogen were measured using an ASAP-2020 (Micromeritics, USA). The specific surface area was calculated using the Brunauer–Emmett–Teller (BET) method and the micropore volumes were calculated using the *t*-plot and Horvath Kawazoe methods. The pore size distribution was calculated based on the density functional theory (DFT). Desilication was measured using solid nuclear magnetic resonance (NMR) spectroscopy (Bruker Avance II 500 MHZ, USA) and FTIR spectroscopy (PerkinElmer Frontier Fourier transform infrared (FTIR) 100, USA).

2.4. Adsorption experiments

Adsorption experiments were carried out using 0.1–1 g of adsorbent in a 30 mL manganese solution (20 and 100 mg/L) at 25°C. The concentration of manganese was determined by UV/vis spectroscopy (Hach, DR 5000, USA) using standard recommended methods (Mn: Periodate Oxidation Method) for examining water.

The adsorption at equilibrium (q_e) at time t and the removal ratio were calculated using the expressions below:

$$q_e = \frac{(C_0 - C_e)V}{W} \tag{1}$$

$$\text{Removal ratio} = \frac{C_t}{C_0} \tag{2}$$

where C_0 is the initial liquid concentration (mg/L), C_e is the equilibrium concentration (mg/L), C_t is the liquid concentration at time t (mg/L), V is the volume of the metal solution (L), and W is the weight of the adsorbent (g).

2.5. Theoretical backgrounds of Langmuir and Freundlich equations

The Langmuir theory describes the monolayer coverage of a solute on an adsorbent surface. The Langmuir isotherm is based on the assumption that adsorption occurs at sites within the adsorbent. The nonlinear form of the Langmuir equation is written as

$$q_e = \frac{\left(q_{m,L} \times K_L C_e\right)}{\left(1 + K_L C_e\right)} \tag{3}$$

where K_L is the Langmuir constant, and $q_{m,L}$ is the adsorption corresponding to the monolayer coverage. In the SigmaPlot 12 equation "Hyperbola equation, Modified Hyperbola I," the form is

$$y = \frac{ax}{\left(1 + bx\right)} \tag{4}$$

The corresponding parameters are $y = q_e$, $a = K_L q_{m,L}$, $b = K_L$, and $x = C_e$.

The Freundlich equation describes the adsorption equilibrium between a solute in the solution and the surface of the adsorbent using a multisite and multilayer concept for a heterogeneous surface [21]. The nonlinear Freundlich form is expressed as

$$q_e = K_F C_e^{1/n_F} \tag{5}$$

where q_e is the adsorption at equilibrium, C_e is the liquid concentration at equilibrium, K_F is the Freundlich constant ((mg/g) (mg/L)) relevant to the adsorption capacity, and $1/n_F$ is the constant related to the adsorption intensity. The corresponding form of the SigmaPlot 12 equation "Power, 2 Parameter" is expressed as

$$y = ax^b \tag{6}$$

The corresponding parameters are $y = q_e$, $a = K_F$, $b = 1/n_F$, and $x = C_e$ [22] (Table 1).

Table 1
Nonlinear and SigmaPlot-fitted forms of the Langmuir and Freundlich equations

Item	Langmuir equation	Freundlich equation
	$Q_e = \frac{\left(q_{m,L} \times K_L C_e\right)}{\left(1 + K_L C_e\right)}$	$Q_e = K_F C_e^{1/n_F}$
SigmaPlot-fitted curve	$Y = \frac{ax}{\left(1 + bx\right)}$	$Y = ax^b$

3. Results and discussion

3.1. Characterization of mesoporous zeolite beta

The development of mesoporosity without severe destruction of essential zeolite properties has been achieved with commercial zeolites via treatment in an alkaline medium and subsequent CTAB assembly. The mesopores of zeolite beta were formed by extracting Si from the framework (desilication) of the commercial material (ZB). The assembly of CTAB, having small beta particles, enables the formation of hierarchical mesopores without the concurrent destruction of the intrinsic zeolite properties. The CTAB assembly and alkaline treatment also open new ways to solve diffusion problems for other applications. The synthesis yields obtained in all experiments ranged from 60% to 70%, considering the total amount of commercial zeolite beta. The resulting materials were designated as MZB-*X*, where *X* denotes the concentration of the NaOH solution used and ZB denoted the commercial zeolite beta.

Fig. 1 presents the XRD patterns of mesoporous zeolite beta (MZB-2, MZB-5, and MZB-7) and compares them with those of a commercial sample (ZB). All mesoporous zeolite beta samples showed a very intense peak at a 2θ = 2°–3° and weak peaks at 2θ = 3°–5°. The three peaks could be indexed to the (100), (110), and (200) planes, indicating a mesostructured hexagonal space group symmetry (p6mm). The intensity of the (100) peak for MZB-7 was much higher than that of the other synthesized mesoporous zeolite samples, possibly due to the higher NaOH concentration, which made the resulting material more homogeneous and subsequently increased its mesoporous ordering. However, in the 2θ region 5°–45°, the peaks due to the beta zeolitic structure of MZB-7 disappeared, especially at 7.6° and 22.4°, indicating severe destruction of the zeolite beta particles after treatment in a 5–7 M NaOH solution. The beta zeolitic structure peaks of MZB-2 were well defined, confirming that MZB-2 consists of beta zeolite having high crystallinity. In the case of MZB-2, the zeolite particles were hydrolyzed into small particles and secondary building units then served as precursors for the synthesis of mesoporous zeolite beta having intrinsic zeolite properties.

The TEM images of MZB-2 are shown in Fig. 2. MZB-2 has random mesopores, in agreement with the results of N_2 sorption isotherms (Fig. 2).

The nitrogen adsorption–desorption isotherms and the related DFT pore size distributions of ZB, MZB-2, MZB-5, and MZB-7 are shown in Fig. 3. The corresponding textural properties obtained from the nitrogen adsorption–desorption isotherms are shown in Table 2.

MZB-2, MBZ-5, and MBZ-7 exhibit IV type isotherms with a sharp nitrogen condensation step at P/P_0 = 0.2–0.4. In particular, MBZ-2 has micropores at 0.7 nm as well as a narrow pore size distribution of about 3.6 nm. As seen in Table 2, the synthesis conditions where the concentration of the NaOH solution is increased also slightly influence the BET surface area. All mesoporous zeolite beta samples have higher surface areas than does the ZB sample. A large surface area typically indicates large adsorption capacity.

ZB shows a microporous volume of 0.2 cm^3/g. The larger mesopores exist owing to process performed by the supplier. These large mesopores do not influence the *t*-plot curve since these pores are larger than 30 nm. The external surface area and mesopore volume are the highest for MZB-7 and decrease at lower NaOH concentrations. Therefore, there is a greater degree of destruction of micropores and generation of mesopores when the zeolite beta is treated with NaOH solutions of higher concentrations.

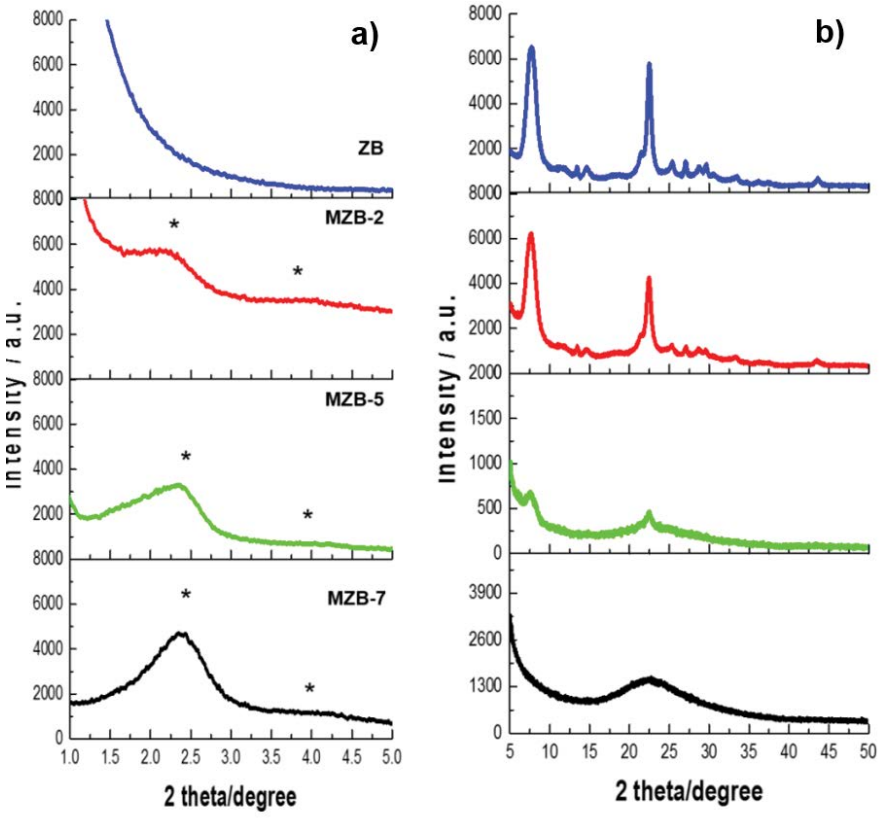

Fig. 1. X-ray diffraction patterns: (a) low angle, (b) high angle of ZB, MZB-2, MZB-5, and MZB-7.

Mesopore formation upon alkaline treatment and CTAB assembly is directly related to the preferential framework from silicon extraction (desilication), leading to decreased Si–O–Si bonding and the destruction of zeolite rings. The breakage and destruction of bonds were confirmed by FTIR spectroscopy (Fig. 4). The results revealed a progressive decrease in the Si–O–Si bending peak at 440–470 and ~1,100 cm^{-1} with increasing concentrations of NaOH. In addition, the bands at 550 and 600 cm^{-1}, which are indicative of zeolite structures in micro/mesoporous zeolite beta, had a lower intensity compared with that of ZB due to the destruction of the zeolite structures when treated with NaOH solutions of higher concentrations.

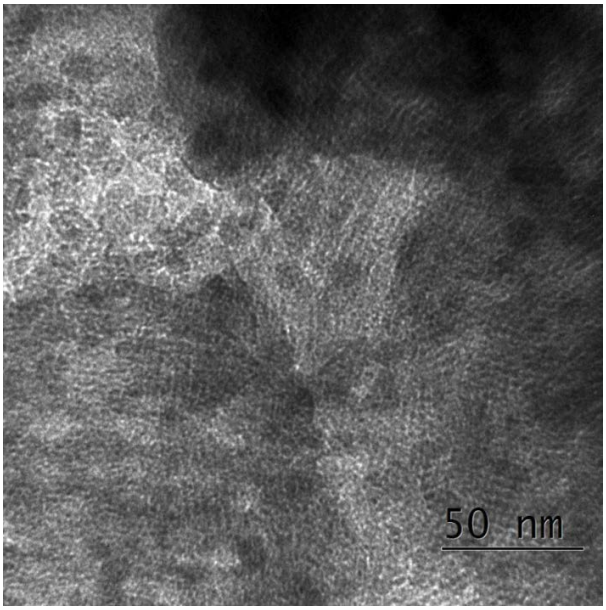

Fig. 2. TEM image of MZB-2.

The ^{29}Si NMR spectra of ZB, MZB-2, MZB-5, and MZB-7 shows a strong signal, which is subsequently assigned to Q_4 (^4Si, ^0Al), and a less intense signal assigned to Q_3 (^3Si, ^1Al) (Fig. 5). The desilication results with 2–7 M NaOH reveal a decrease in the intensity of Q_4 due to a decrease in the Si/Al ratio of zeolite beta by desilication, whereas the Q_3 signal changes minimally. The difference in the change between the Q_4 and Q_3 unit signals is because the Q_4 unit is the first to be extracted during the alkaline treatment [23].

3.2. Adsorption of manganese by natural and modified zeolites

The adsorption capacities of ZB and the mesoporous zeolite betas, MZB-2 and MZB-7, are shown in Fig. 6.

The adsorption of Mn^{2+} was performed over 40 min for ZB, MZB-2, and MZB-7 in a 100 ppm Mn solution. All the mesoporous zeolite beta exhibited higher adsorption capacity than ZB. Overall, MZB-2 displayed the highest adsorption capacity among the adsorbents despite having a lower surface area than that of MZB-5 and MZB-7. The zeolite characteristics of MZB-2 facilitated the adsorption and diffusion of Mn^{2+}

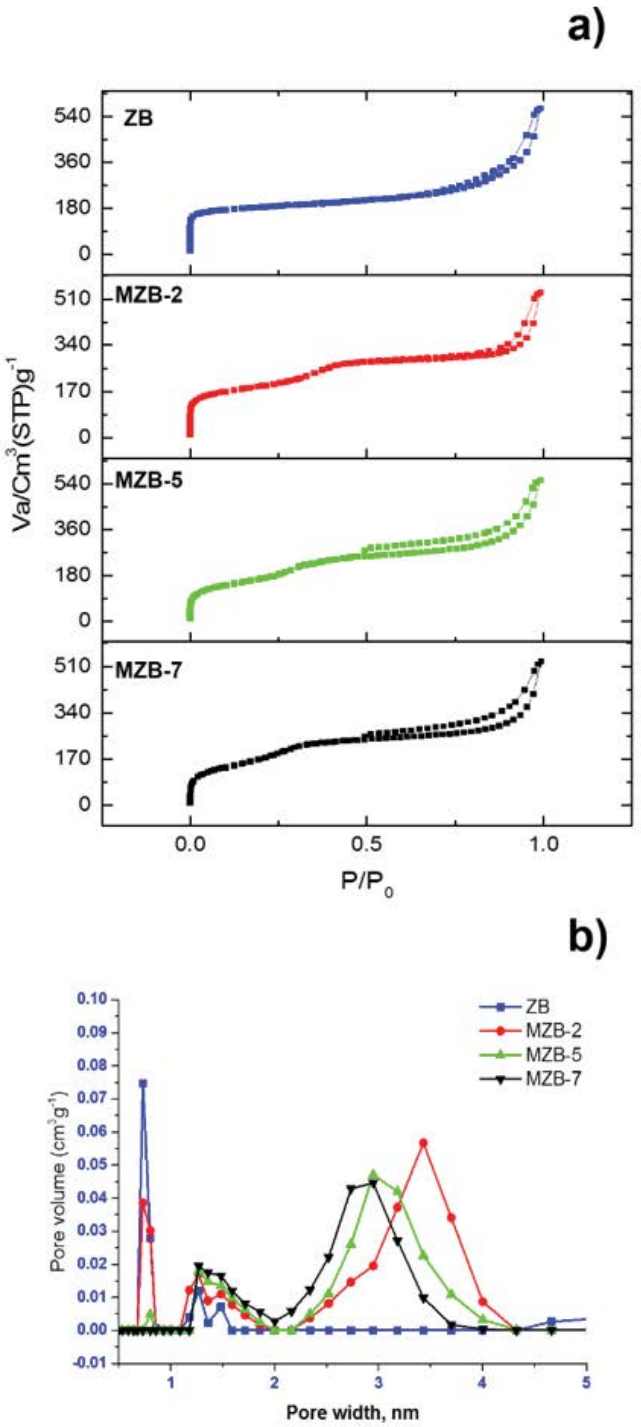

Fig. 3. (a) Nitrogen adsorption–desorption isotherms and (b) DFT pore size distribution of ZB, MZB-2, MZB-5, and MZB-7.

via ion exchange. A high NaOH concentration (> 5 M) led to structural deformation and serious destruction of the zeolite characteristics, as seen in Fig. 3 and Table 2. The adsorption of Mn^{2+} was performed over 40 min for MZB-2, and MZB-7 in a 20 ppm Mn solution. Removal ratio and Q_e value for Mn^{2+} depending on different dosages of MBZ-2 and MBZ-7 are shown in Fig. 7.

Table 2
Textural parameters of ZB, MZB-2, MZB-5, and MZB-7

	NaOH concentration (M)	S_{BET} (m^2/g)	S_{ext} (m^2/g)	V_{micro} (cm^3/g)	V_{total} (cm^3/g)
ZB	–	601	231	0.2	0.88
MZB-2	2	657	479	0.08	0.82
MZB-5	5	656	635	0.02	0.85
MZB-7	7	660	639	0.01	0.81

Based on the results in Fig. 7, the Langmuir and Freundlich models were fitted to the adsorption isotherms. The adsorption constants obtained from these isotherms are given in Table 3. The Freundlich model is, therefore, deemed suitable for Mn removal using MBZ-2 as opposed to MBZ-7.

In Fig. 7, the points were fitted using the SigmaPlot 12 "Hyperbola equation, Modified Hyperbola I" fitting. Based on calculations from the Langmuir model (Fig. 8), the manganese adsorption capacities were 10.3 and 9.9 mg/g for MZB-2 and MZB-7, respectively, and the K_L values were 0.61 and 0.12. The high K_L value indicates a high binding affinity for MZB-2 and Mn^{2+}. The points from Fig. 7 were also fitted using SigmaPlot 12 "Power, 2 Parameter" fitting. The k_F value was found using the Freundlich isotherms, which represents the adsorption capacity estimated from the equation. A larger k_F value indicates a better adsorption capacity. Here, the $1/n_F$ values indicate the adsorption strength; if the value is between 0 and 1, the adsorption is good. In Fig. 7, the $1/n_F$ values for MZB-2 and MZB-7 are both in the range of 0–1, showing a strong adsorption capacity, as reported in Ref. [24].

The adsorption capacity and affinity of MZB-2 for Mn^{2+} are higher than those of NZ [25] obtained from Manisa-Demirci (51% clinoptilolite, 12% dolomite, 4% quartz, 17% feldspar, and 9% biotite), whereas the corresponding values for MZB-7 are slightly lower. These differences may be related to the mesoporosity as well as the presence of zeolite characteristics and the porosity of the adsorbents.

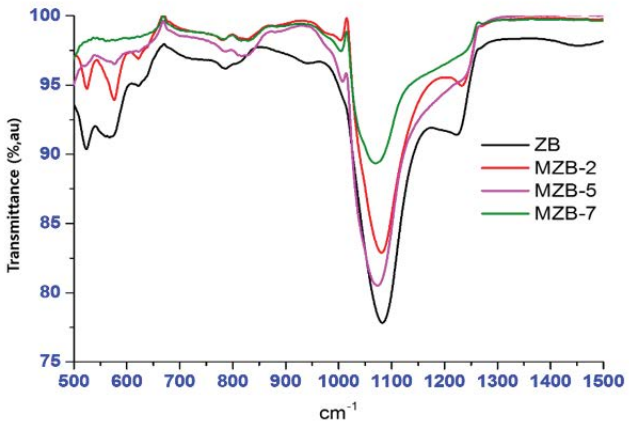

Fig. 4. FTIR study of ZB, MZB-2, MZB-5, and MZB-7.

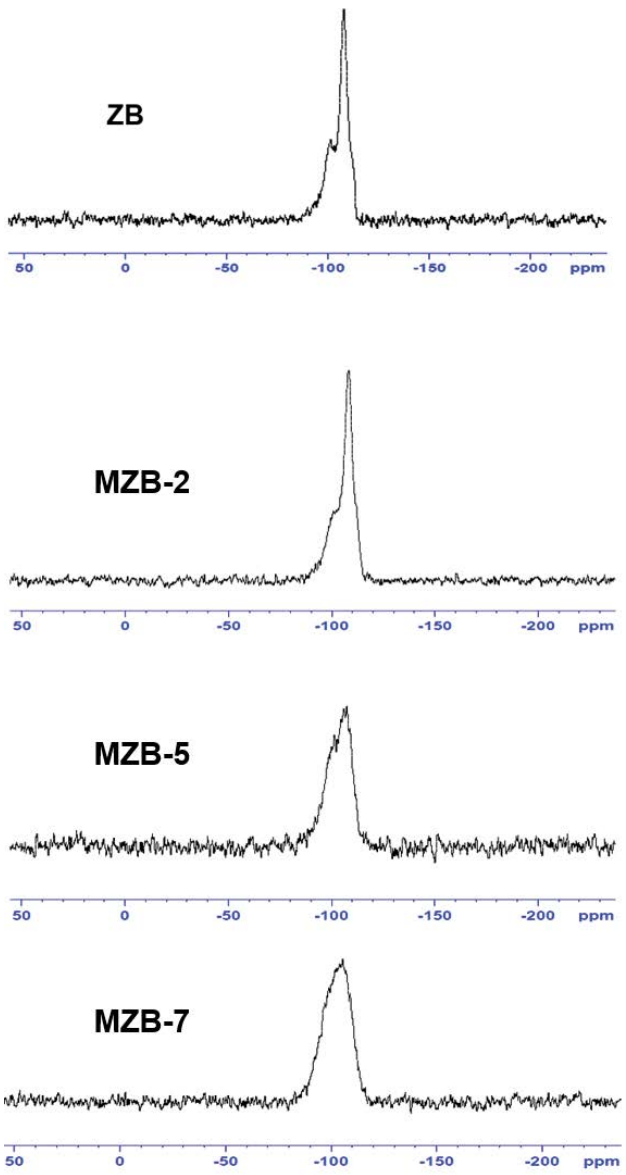

Fig. 5. ^{29}Si NMR spectra of ZB, MZB-2, MZB-5, and MZB-7.

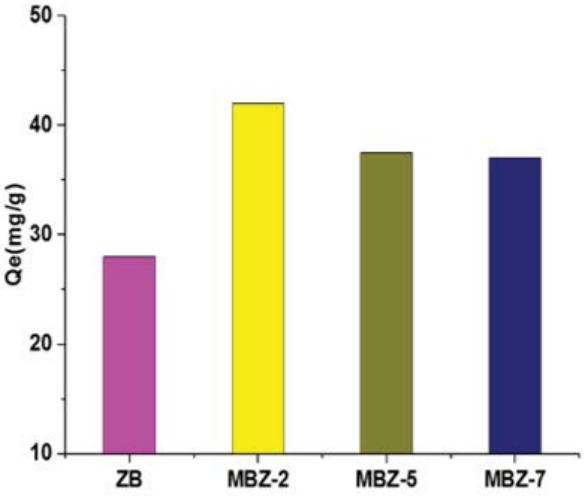

Fig. 6. The Q_e value depending on different adsorbents (concentration: 100 ppm; contact time: 40 min; ZB, MZB-2, MZB-5, and MZB-7).

4. Conclusion

In this study, mesoporous zeolite beta was prepared by desilication with NaOH and reassembly with CTAB, and the adsorption capacity for manganese was investigated. The following were confirmed: (1) The pore size and crystallinity of mesoporous zeolite beta were investigated by XRD patterns. It was found that the mesoporous zeolite beta synthesized by treatment with 2 M NaOH had clear zeolite crystallinity and mesoporosity; (2) In the 100 ppm Mn solution, the q_e values of ZB, MZB-2, MZB-5 and MZB-7 were 26.5, 42, 37.5, and 35.6 mg/g, respectively; (3) The adsorption characteristics of MZB-2 were especially well explained by the Freundlich isothermal adsorption model; (4) It was confirmed that the Mn adsorption performance was improved with the use of mesoporous zeolite beta; (5) Finally, an adsorbent having excellent performance can be produced by NaOH treatment during the synthesis of mesoporous zeolite beta.

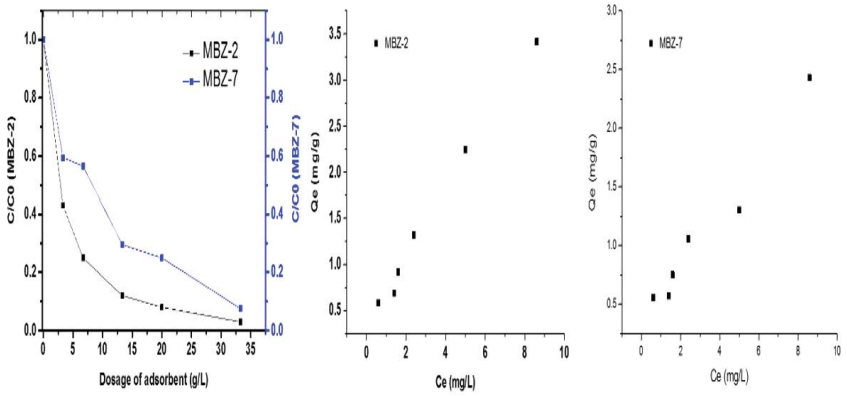

Fig. 7. Removal ratio [+] and plot of Q_e versus C_e for Mn^{2+} depending on different dosages of MBZ-2 and MBZ-7 (concentration: 20 ppm; contact time: 40 min).

Table 3
Parameters calculated from Langmuir and Freundlich isotherm models

Langmuir equation	MBZ-2	MBZ-7	NZ [25]	Freundlich equation	MBZ-2	MBZ-7	NZ
K_L (L/mg)	0.61	0.12	0.08	$1/n_F$	0.73	1.01	0.9
$q_{m,L}$ (mg/g)	10.32	9.92	7.1	K_F	0.69	0.15	0.02
R	0.99	0.85		R	0.99	0.85	–

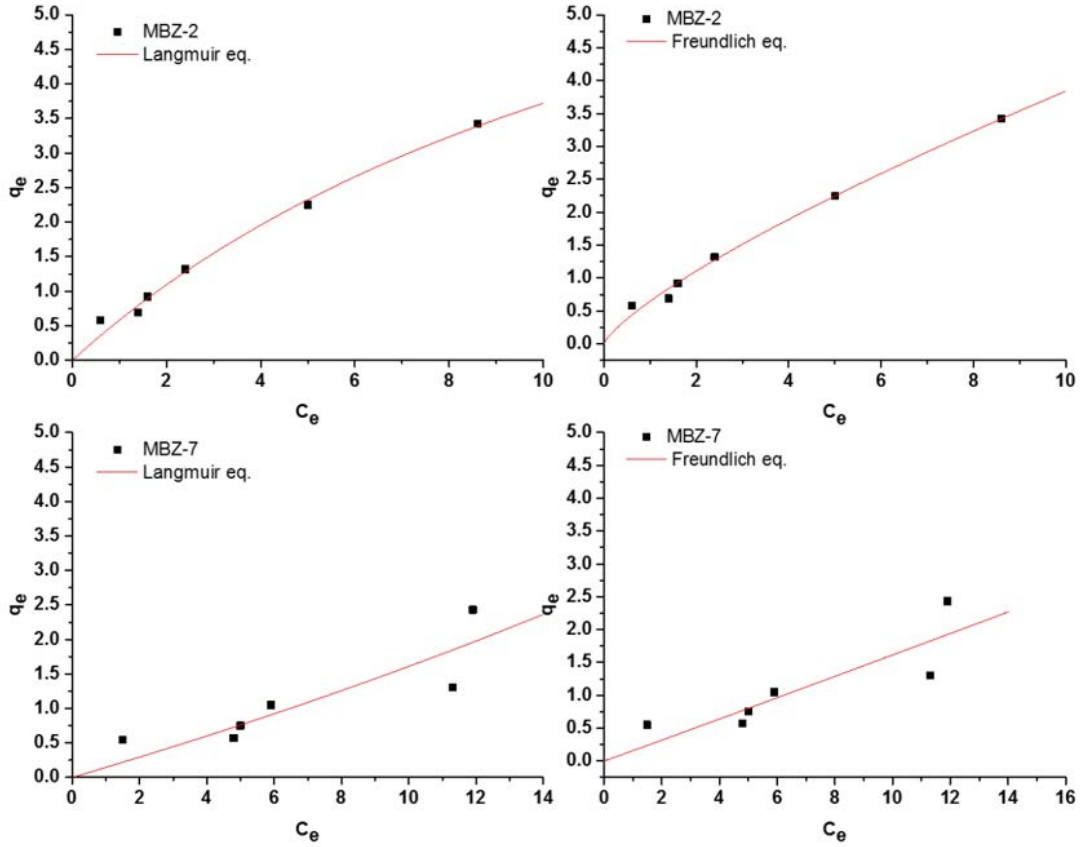

Fig. 8. Langmuir isotherm plot and Freundlich plot of MBZ-2 and MBZ-7 obtained by changing adsorbent dosage.

Acknowledgment

This subject is supported by ICMTC and ADD (16-SF-2B-14) and a grant (17CTAP-C133297-01) from infrastructure and transportation technology promotion research program funded by ministry of Land, Infrastructure and Transport of Korean government.

References

[1] D. Ellis, C. Bouchard, G. Lantagne, Removal of iron and manganese from groundwater by oxidation and microfiltration, Desalination, 130 (2007) 255–264.
[2] A. Alpatova, S. Verbych, M. Bryk, R. Nigmatullin, N. Hilal, Ultrafiltration of water containing natural organic matter: heavy metal removing in the hybrid complexation–ultrafiltration process, Sep. Purif. Technol., 40 (2004) 155–162.
[3] B.A.M. Al-Rashdi, D.J. Johnson, N. Hilal, Removal of heavy metal ions by nanofiltration, Desalination, 315 (2013) 2–17.
[4] S. Wang, Y. Peng, Natural zeolites as effective adsorbents in water and wastewater treatment, Chem. Eng. J., 156 (2010) 11–24.
[5] J. Pérez-Ramírez, F. Kapteijn, J.C. Groen, A. Doménech, G. Mul, J.A. Moulijn, Steam-activated FeMFI zeolites. Evolution of iron species and activity in direct N_2O decomposition, J. Catal., 214 (2003) 33–45.
[6] I.I. Ivanova, E.E. Knyazeva, Micro-Mesoporous materials obtained by zeolite recrystallization: synthesis, characterization and catalytic application, Chem. Soc. Rev., 42 (2013) 3671–3688.
[7] M. Müller, G. Harvey, R. Prins, Comparison of the dealumination of zeolites beta, mordenite, ZSM-5 and ferrierite by thermal treatment, leaching with oxalic acid and treatment with $SiCl_4$ by ^1H, ^{29}Si and ^{27}Al MAS NMR, Microporous Mesoporous Mater., 34 (2000) 135–147.
[8] R.M. Dessau, E.W. Valyocsik, N.H. Goeke, Aluminum zoning in ZSM-5 as revealed by selective silica removal, Zeolites, 12 (1992) 776–779.
[9] R. Le Van Mao, S.T. Le, D. Ohayon, F. Caillibot, L. Gelebart, G. Denes, Modification of the micropore characteristics of the desilicated ZSM-5 zeolite by thermal treatment, Zeolites, 19 (1997) 270–278.
[10] M. Ogura, S. Shinomiya, J. Tateno, Y. Nara, E. Kikuchi, M. Matsukata, Formation of uniform mesopore in ZSM-5

zeolite through treatment in alkaline solution, Chem. Lett., 29 (2000) 882–883.
[11] M. Ogura, S. Shinomiya, J. Tateno, Y. Nara, M. Nomura, E. Kikuchi, M. Matsukata, Alkali-treatment technique – new method for modification of structural and acid-catalytic properties of ZSM-5 zeolites, Appl. Catal., A, 219 (2001) 33–43.
[12] T. Suzuki, T. Okuhara, Change in pore structure of MFI zeolite by treatment with NaOH aqueous solution, Microporous Mesoporous Mater., 43 (2001) 83–89.
[13] J.C. Groen, J. Pérez-Ramírez, L.A.A. Peffer, Formation of uniform mesoporous in ZSM-5 zeolite upon alkaline post treatment? Chem. Lett., 31 (2002) 94–95.
[14] P. Losch, T.C. Hoff, J.F. Kolb, C. Bernardon, J.P. Tessonnier, B. Louis, Mesoporous ZSM-5 zeolites in acid catalysis: top-down vs. bottom-up approach, Catalysts, 7 (2017) 225–243.
[15] K.P. de Jong, J. Zečević, H. Friedrich, P.E. de Jongh, M. Bulut, S. van Donk, R. Kenmogne, A. Finiels, V. Hulea, F. Fajula, Zeolite Y crystals with trimodal porosity as ideal hydrocracking catalysts, Angew. Chem., Int. Ed., 49 (2010) 10074–10078.
[16] S. Wang, T. Dou, Y. Li, Y. Zhang, X. Li, Z. Yan, A novel method for the preparation of MOR/MCM-41 composite molecular, Catal. Commun., 6 (2005) 87–91.
[17] S.V. Konnov, I.I. Ivanova, O.A. Ponomareva, V.I. Zaikovskii, Hydroisomerization of n-alkanes over Pt-modified micro/mesoporous materials obtained by mordenite recrystallization, Microporous Mesoporous Mater., 164 (2012) 222–231.
[18] I.A. Kasyanov, A.A. Maerle, I.I. Ivanova, V.I. Zaikovskii, Towards understanding of the mechanism of stepwise zeolite recrystallization into micro/mesoporous materials, J. Mater. Chem. A, 2 (2014) 16978–16988.
[19] V.V. Ordomsky, V.Y. Murzin, Y.V. Monakhova, Y.V. Zubavichus, E.E. Knyazeva, N.S. Nesterenko, I.I. Ivanova, Nature, strength and accessibility of acid sites in micro/mesoporous catalysts obtained by recrystallization of zeolite BEA, Microporous Mesoporous Mater., 105 (2007) 101–110.
[20] Y. Li, W. Zhang, X. Wang, Y. Zhang, T. Dou, K. Xie, Synthesis, characterization, and catalytic properties of a hydrothermally stable Beta/MCM-41 composite from well-crystallized zeolite Beta, J. Porous Mater., 15 (2008) 133–138.
[21] A. Gil, F.C.C. Assis, S. Albeniz, S.A. Korili, Removal of dyes from wastewaters by adsorption on pillared clays, Chem. Eng. J., 168 (2011) 1032–1040.
[22] F.C. Wu, P.-H. Wu, R.-L. Tseng, R.-S. Juang, Use of refuse-derived fuel waste for the adsorption of 4-chlorophenol and dyes from aqueous solution: equilibrium and kinetics, J. Taiwan Inst. Chem. Eng., 45 (2014) 2628–2639.
[23] K. Tarach, K. Góra-Marek, J. Tekla, K. Brylewska, J. Datka, K. Mlekodaj, W. Makowski, M.C. Igualada López, J. Martínez Triguero, F. Rey, Catalytic cracking performance of alkaline-treated zeolite Beta in the terms of acid sites properties and their accessibility, J. Catal., 312 (2014) 46–57.
[24] H. Kim, M.E. Lee, S. Kang, J.W. Chung, Thermodynamic analysis of phenol adsorption by powdered activated carbon, J. Korean Soc. Environ. Eng., 35 (2013) 220–225.
[25] Y.T. Kim, K.D. Jung, E.D. Park, Gas-phase dehydration of glycerol over ZSM-5 catalysts, Microporous Mesoporous Mater., 131 (2010) 28–36.